

1 **Epigenetic and genetic population structure is coupled in a marine**
2 **invertebrate**

3 Katherine Silliman^{1§}, Laura H. Spencer^{2§}, Samuel J. White², Steven B. Roberts^{2*}

4 ¹Marine Resources Research Institute, South Carolina Department of Natural Resources,
5 Charleston, SC 29412, USA

6 ²School of Aquatic and Fishery Sciences, University of Washington, Seattle, WA, USA

7 [§]denotes equal author contribution

8 ^{*}denotes coresponding author

9 **Abstract**

10 Delineating the relative influence of genotype and the environment on DNA methylation
11 is critical for characterizing the spectrum of organism fitness as driven by adaptation and
12 phenotypic plasticity. In this study, we integrated genomic and DNA methylation data for two
13 distinct Olympia oyster (*Ostrea lurida*) populations while controlling for within-generation
14 environmental influences. In addition to providing the first characterization of genome-wide DNA
15 methylation patterns in the oyster genus *Ostrea*, we identified 3,963 differentially methylated loci
16 between populations. Our results show a clear coupling between genetic and epigenetic
17 patterns of variation, with 27% of variation in inter-individual methylation differences explained
18 by genotype. Underlying this association are both direct genetic changes in CpGs (CpG-SNPs)
19 and genetic variation with indirect influence on methylation (mQTLs). The association between
20 genetic and epigenetic patterns breaks down when comparing measures of population
21 divergence at specific genomic regions, which has implications for the methods used to study
22 epigenetic and genetic coupling in marine invertebrates.

23 *Keywords: oyster, DNA methylation, single nucleotide polymorphism, Ostrea, environment,*
24 *epigenetic*

25 Significance statement

26 We know that genotype and epigenetic patterns are primarily responsible for phenotype,
27 yet there is a lack of understanding to what degree the two are linked. Here we characterized
28 the mechanisms and the degree by which genetic variation and DNA methylation variation are
29 coupled in a marine invertebrate, with almost a third of the methylation variation attributable to
30 genotype. This study provides a framework for future studies in environmental epigenetics to
31 take genetic variation into account when teasing apart the drivers of phenotypic variation. By
32 identifying methylation variation that cannot be attributed to genotype or environmental changes
33 during development, our results also highlight the need for future research to characterize
34 molecular mechanisms adjacent to genetic adaptation for producing long-term shifts in
35 phenotype.

36 Introduction

37 It is increasingly evident that epigenetic processes both influence phenotype and interact
38 with genetic variation. One such epigenetic process is DNA methylation, which commonly refers
39 to the methylation of a cytosine in a CpG dinucleotide. The role of DNA methylation is diverse
40 across taxa and varies based on the genomic location. In most vertebrates, DNA methylation is
41 widespread across the genome and silences transcriptional activity when present in the
42 promoter regions (Wagner et al. 2014; Zemach et al. 2010; Varriale 2014). In contrast many
43 marine invertebrates have sparsely methylated genomes and the influence of methylation on
44 transcription is more complex (Suzuki & Bird 2008; Roberts & Gavery 2012; de Mendoza et al.
45 2019). In both vertebrates and invertebrates, the removal and addition of methyl groups can

46 become canalized during the lifetime of that organism, and if occurring in germ cells has the
47 potential to influence subsequent generations. This heritability of DNA methylation, as well as
48 taxa-specific methylation rates and patterns, suggest that methylation differences arose in part
49 due to evolutionary forces (Varriale 2014).

50 While the patterns and functions of CpG methylation differ among vertebrate and
51 invertebrate taxa, in both systems methylation is highly variable. The evolutionary source of this
52 variation is now an area of active research, with the two dominant factors appearing to be 1) an
53 organism's environmental history (intra- and inter-generational), and 2) its genotype (Jaenisch &
54 Bird 2003; Lienert et al. 2011; Danchin et al. 2011). Understanding how the environment and
55 genotype interact to influence DNA methylation is critical for delineating organism fitness as
56 driven by phenotypic plasticity and adaptation, particularly in the context of global climate
57 change. Bivalves, and oysters in particular, are a valuable model for investigating invertebrate
58 methylation patterns due to their experimental tractability and concordant development of
59 genomic resources (Timmins-Schiffman et al. 2013).

60 DNA methylation has been shown to vary in response to environmental factors in marine
61 invertebrates (Eirin-Lopez & Putnam 2019). In oysters, differential methylation has been
62 reported in response to ocean acidification (Lim et al. 2020; Downey-Wall et al. 2020), salinity
63 stress (Xin Zhang et al. 2017), air exposure (X. Zhang et al. 2017), and the herbicide diuron
64 (Akcha et al. 2020). Because there are clear associations between methylation and
65 transcriptional activity (Gavery & Roberts 2013; Olson & Roberts 2014; Rivière 2014; Johnson
66 et al. 2020; Song et al. 2017), methylation changes may contribute to phenotypic plasticity in
67 response to abiotic stressors (Venkataraman et al. 2020; Wang et al. 2021a; Lim et al. 2020;
68 Gonzalez-Romero et al. 2017; Wang et al. 2020; Downey-Wall et al. 2020). Methylation
69 changes triggered by the environment may themselves be heritable if they occur in gametes,
70 leading to transgenerational plasticity. It is the dynamic characteristics of the methylome that is

71 fueling a growing body of research associating methylation variation with environmental
72 exposures, particularly in trans-generational studies (Eirin-Lopez & Putnam 2019). However,
73 few studies have controlled for (or described) the relationship between methylotype and
74 genotype in test organisms (but see (Wang et al. 2021b; Johnson & Kelly 2020; Kvist et al.
75 2018), likely because in non-model taxa there is limited understanding of how the methylome is
76 shaped by the genome.

77 While efforts to explore the influence of genotype on DNA methylation are limited in
78 marine invertebrates, studies in taxa with advanced genomic resources have identified
79 associations between genetic variants and DNA methylation (Banovich et al. 2014; Taudt et al.
80 2016). In oysters, genes with constitutive high levels of methylation have less genetic variation
81 within populations (Roberts & Gavery 2012). Similar results have been found in the coral *Apis*
82 *mellifera* and the jewel wasp (*Nasonia vitripennis*)(Lyko et al. 2010)(Park et al. 2011). One direct
83 mechanism by which genetic and epigenetic variation can be associated are single nucleotide
84 polymorphisms (SNPs) that create or remove CpG loci (CpG-SNPs), and therefore can
85 immediately affect local methylation status (Shoemaker et al. 2010; Zhi et al. 2013).
86 Alternatively, methylation status itself may change the likelihood of a SNP from occurring by
87 “shielding” genetic mutations from selection, allowing genetic differentiation to accumulate
88 (Klironomos et al. 2013), and by changing rates of homologous recombination (Li et al. 2012)
89 and copy number variation mutation (discussed in (Skinner et al. 2014)). Surprisingly, some
90 recent studies in oysters have found no relationship between genetic and epigenetic
91 differentiation among populations or breeding cohorts, resulting in the suggestion that these two
92 processes are uncoupled (Johnson & Kelly 2020; Jiang et al. 2013; Wang et al. 2020).

93 Genetic changes that are associated with methylation state but located some distance
94 from the associated CpG are referred to as methylation quantitative trait loci (mQTLs). In
95 humans, mQTLs may contribute up to 15-20% of inter-individual variation in methylation and up

96 to 70% of population-level methylation variation (Heyn et al. 2013; McClay et al. 2015; Husquin
97 et al. 2018; van Dongen et al. 2016). These genetic and epigenetic variants are often
98 associated with complex traits or environmental differences, such as immunity or history of
99 tobacco exposure (Gao et al. 2017; Bonder et al. 2017; McClay et al. 2015). Mechanistically,
100 mQTLs have been proposed to operate in a number of ways. Global methylation patterns can
101 be influenced by changing the expression or activity of methyltransferases, although mQTLs are
102 rarely found in these genes. Increasingly, transcription factors and their binding sites have been
103 implicated with mQTLs, as transcription factor binding can prevent methylation of nearby CpGs
104 (Héberlé & Bardet 2019). Under this model, genetic variants in transcription factor binding sites
105 can influence local methylation (local mQTLs), while genetic variants that affect the activity of
106 wide-acting transcription factors can influence methylation at many distant CpGs near binding
107 sites for that specific transcription factors (distant mQTLs). While these mechanisms have not
108 been investigated in most non-model taxa, the conserved roles of transcription factors across
109 taxa suggests that they may also play a role in shaping methylation variation in invertebrates
110 and bivalves (Nitta et al. 2015; Bell et al. 2011). Functional genomics are needed to further
111 investigate these relationships to ascertain the mechanisms underlying genetic and epigenetic
112 relationships in nonmodel taxa.

113 The Olympia oyster (*Ostrea lurida*) is an emerging model taxa for investigating the links
114 between environment, genetic adaptation, and epigenetic plasticity (White et al. 2017; Silliman
115 2019; Maynard et al. 2018; Timmins-Schiffman et al. 2013). Native to estuaries from Baja
116 California to the central coast of Canada, *O. lurida* extends over strong environmental clines
117 and mosaics (Chan et al. 2017; Schoch et al. 2006). Significant neutral and putatively adaptive
118 genetic variation has been detected between populations at both regional and local scales,
119 which is surprising given the potential for high connectivity during the planktonic larval phase
120 (Silliman 2019). Experimental tests for local adaptation among neighboring sites within San

121 Francisco Bay, CA (Maynard et al. 2018) and Puget Sound, WA (Silliman et al. 2018; Heare et
122 al. 2017) have found phenotypic variation at fitness-related traits, such as growth, salinity
123 tolerance, and reproductive timing. By controlling for environmental variation, these studies
124 suggest a strong heritable component underlying population differences. Whether this
125 component is due to genetic variation, inherited epigenetic modifications, or a combination is
126 still unknown.

127 The objective of the current study was to leverage a new *O. lurida* draft genome to
128 investigate the relationship between CpG methylation and genetic variation based on 2b-RAD SNPs.
129 Oysters from two populations in Puget Sound, WA were raised to maturity for one generation in
130 common conditions to remove lifetime exposure to environmental variation. These populations
131 have phenotypic variation in larval and adult size and reproductive timing (Silliman et al. 2018;
132 Heare et al. 2017; Spencer et al. 2020), show varied gene expression profiles under stress
133 (Heare et al. 2018), and come from sites with different environmental profiles in dissolved
134 oxygen, temperature, pH, salinity, and food availability (Moore et al. 2008; Banas et al. 2015;
135 Khangaonkar et al. 2018). While some marine invertebrate studies have associated overall
136 patterns of epigenetic and genetic differentiation between populations (e.g., (Johnson & Kelly
137 2020), to our knowledge this is the first to directly link epigenetic and genetic variability by
138 identifying and functionally characterizing CpG-SNPs and meth-QTLs.

139 Results

140 Study Design

141 Adult Olympia oysters (*O. lurida*) derived from two separate parent populations in Puget
142 Sound, Washington were reared in Clam Bay, Washington. The two parental populations were

143 from Hood Canal and South Sound. Details on broodstock collection and outplanting are
144 described in (Heare et al. 2017). Shell length and wet weight were measured immediately prior
145 to adductor tissue dissection. Biallelic SNPs were genotyped in 114 individuals (57 from each
146 population) using a reduced-representation 2b-RAD approach (Wang et al. 2012) by mapping to
147 a draft *O. lurida* genome assembly (GCA_903981925.1) (159,429 scaffolds, N50 = 12,947).
148 After filtering for sample coverage (at least 3 reads in >70% of individuals) and a minimum
149 overall minor allele frequency (MAF) of 0.01, genotype likelihoods were calculated with ANGSD
150 for 5,269 SNPs and used for subsequent population genetic analyses (Korneliussen et al.
151 2014).

152 To characterize CpG methylation patterns, we randomly selected 9 genotyped
153 individuals from each population and used methyl-CpG binding domain (MBD) bisulfite
154 sequencing (MBD-BS). These 18 samples are referred to as the MBD18 samples. This reduced
155 representation approach is efficient for taxa with sparse methylation patterns, as it enriches for
156 methylated DNA regions while providing single base resolution through bisulfite conversion
157 (Trigg et al. 2021). Reads from all MBD18 samples were concatenated into one 'meta-sample'
158 and aligned to the *O. lurida* genome to describe general methylation patterns in the Olympia
159 oyster. Out of 2,030,624 CpG loci with at least 5x sequencing coverage in the 'meta-sample',
160 1,839,241 (90.6%) were methylated, defined as loci with greater than 50% of reads remaining
161 cytosines after bisulfite conversion.

162 For comparative methylation analyses, reads from each MBD18 sample were aligned
163 separately, and a more conservative set of 252,115 loci were used by filtering for loci with 5x
164 coverage across at least 7 of the 9 samples within each population. As MBD-BS enriches for
165 methylated regions, this conservative filtering approach may exclude regions that were
166 methylated in one population but largely unmethylated in the other. Therefore, we included an
167 additional 251 CpG loci that were minimally sequenced in one population (≤ 1 sample) and

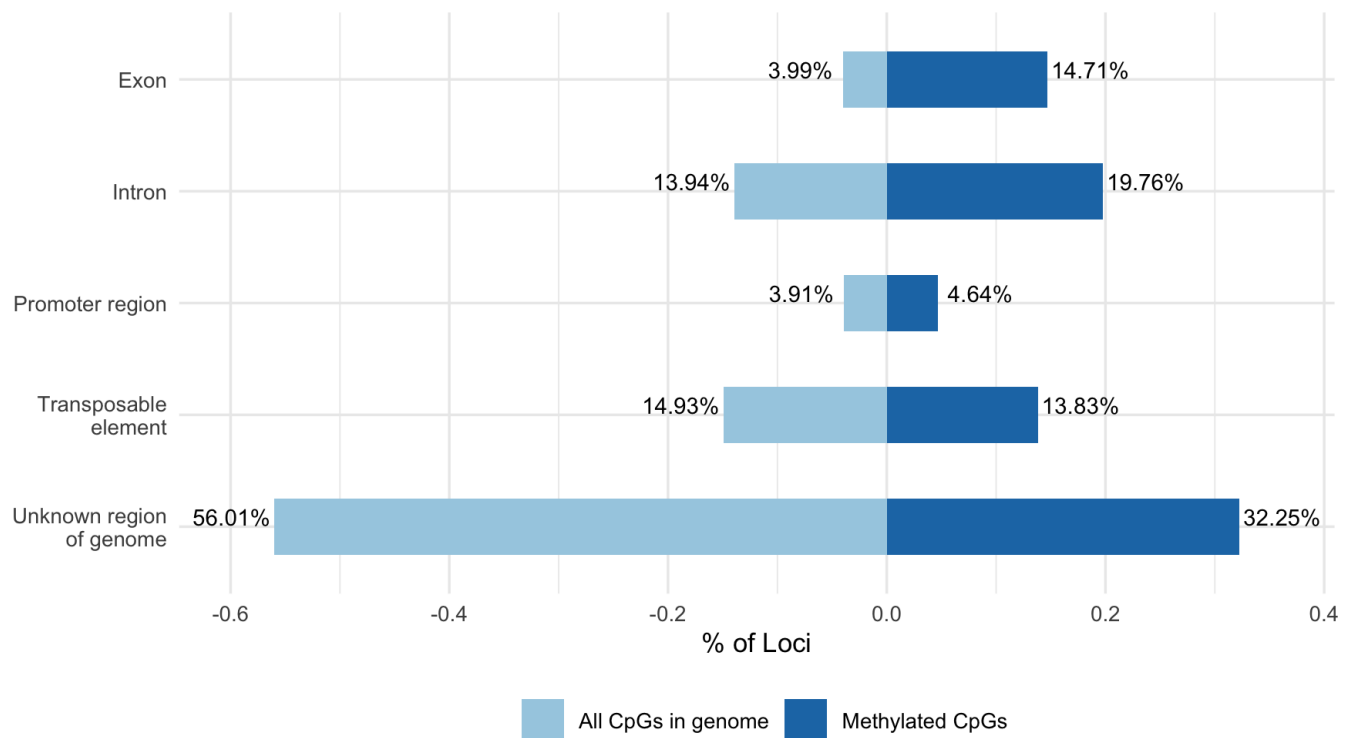
168 widely sequenced in the other population (≥ 7 samples), and annotated samples with missing
169 data in the low-sequenced population as unmethylated at 5x coverage.

170 Genome annotation and general methylation landscape

171 The draft genome assembly (Accession # GCA_903981925.1) is 1.1 Gb in size with a
172 contig N50 of 7.8kb. Gene prediction identified 32,210 genes, 170,394 exons, and 163,637
173 coding sequences. Additionally, 27,331,887 CpG motifs were identified in the genome
174 assembly.

175 Transposable element identification determined GC content of the genome to be
176 36.58%. Retroelements comprised 6.24% of the genome assembly. Those retroelements
177 consisted of 0.03% small interspersed nuclear elements (SINEs), 5.69% long interspersed
178 nuclear elements (LINEs), and 0.53% of long terminal repeat (LTR) elements. DNA transposons
179 made up 3.13% of genome assembly.

180 Of the 27,331,887 CpGs in the *O. lurida* genome we found that 1,839,241 were
181 methylated (6.73%) using the concatenated MBD18 reads. Of the 1,839,241 methylated loci
182 34.5% were intragenic (14.7% in exons, 19.8% in introns), 4.6% and 4.7% were located 2kb
183 upstream and downstream of known genes, respectively, and 13.8% were within transposable
184 elements. 32.3% of the methylated loci were not associated with known regions (i.e. intergenic
185 beyond 2kb gene flanking regions) (Figure 1). The distribution of methylated loci across
186 genomic features differed significantly from the distribution of all CpG loci in the *O. lurida*
187 genome ($\chi^2=685,890$, $df=5$, $p=0$), and methylated CpG loci were $\sim 3.7x$ more likely to be located
188 within an exon (Supplemental Figure 2).

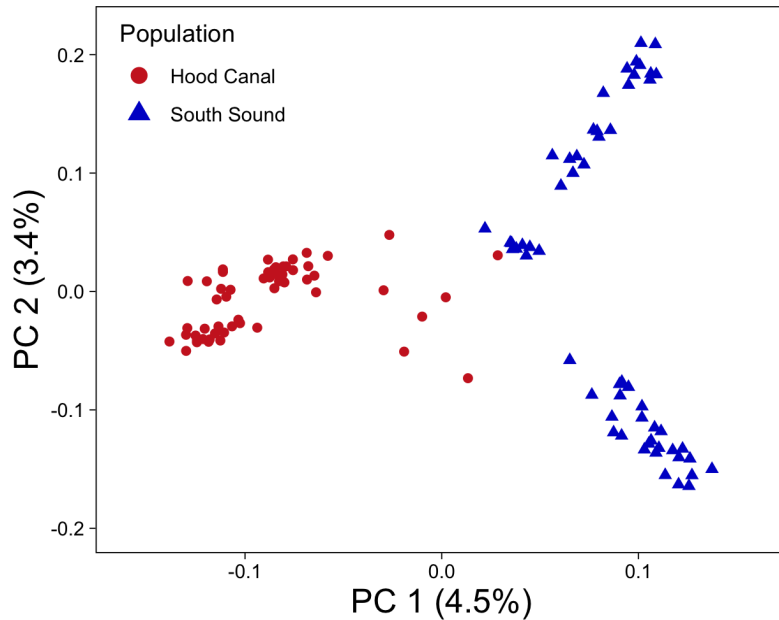


189 **Figure 1:** Comparison of the percentages of CpGs in genome (light blue) vs. methylated CpG loci (dark
 190 blue) in *O. lurida* muscle tissue that intersect with each of the following genomic features: exon, intron,
 191 promoter region (within 2kb of the 5' end of a gene), transposable element, unknown region of genome.
 192 Compared to all CpGs in the *O. lurida* genome methylated loci are more likely to be located in exons
 193 (3.7x) and introns (1.4x), and less likely to be located in unknown regions (0.60x).

194 Population genetic structure

195 Population genetic analyses of all 114 individuals found evidence of divergence with
 196 gene flow between the two populations. Principal component analysis (PCA) of 5,269 SNPs
 197 clustered individuals primarily by population of origin along PC1, which represented 6.64% of
 198 the total variation (Figure 2). NGSadmix was used to perform an ADMIXTURE analysis based
 199 on genotype likelihoods of 3,724 SNPs, after filtering further for a minimum overall allele
 200 frequency of 0.05 (Skotte et al. 2013). The most likely number of genetic clusters (K) was
 201 determined to be K = 2, with evidence of admixture between the two sampled populations

202 (Supplemental Figure 7). Outlier analyses with BayeScan detected 12 SNPs as potentially
203 under divergent selection (Foll & Gaggiotti 2008). One of these SNPs was found in a gene
204 involved in cell mitosis (G2/mitotic-specific cyclin-B) and another was within 2kb downstream of
205 a gene involved in protein ubiquitination (SOCS5) (Supplemental Table 3).



206 **Figure 2:** PCA based on 5,269 SNPs for 114 individuals, with colors and shape referring to parental
207 population.

208 Population genetic differentiation (F_{ST}) was measured overall and separately for each
209 SNP and each gene region (\pm flanking 2 kb) (Reynolds et al. 1983). These values were derived
210 from estimates of the site-frequency spectrum (SFS) in ANGSD, and therefore used 5,882
211 SNPs that were filtered as to avoid distorting the allele frequency spectrum (Korneliussen et al.
212 2014). Overall unweighted F_{ST} between the two populations was 0.0596 (SD=0.087), and
213 weighted F_{ST} was 0.0971. Per-SNP F_{ST} was calculated for 5,882 SNPs, with 1,909 of these SNPs
214 found across 1,386 genes. Mean F_{ST} for SNPs in genes was slightly lower than overall F_{ST} with
215 an unweighted F_{ST} of 0.0586 (SD=0.084) and weighted F_{ST} of 0.093. 38 genes had an $F_{ST} > 0.3$,

216 and were enriched for four biological processes, including steroid hormone mediated signaling
217 pathway and three processes related to autophagy (Supplemental Table 4).

218 DNA methylation differences between populations

219 Population methylation analyses of the MBD18 individuals found evidence of epigenetic
220 divergence. Principal component analysis, which was performed on a percent methylation
221 matrix (252,366 loci x 18 samples), clustered individuals by population of origin along PC2,
222 which represented 8.5% of the total variation (Figure 3b). Logistic regression analysis identified
223 3,963 differentially methylated loci between populations (DMLs, methylation difference >25%
224 and Q-value <0.01, Supplemental Figure 4), 1,915 of which were located within known genes
225 (48.3% of DMLs), and 1,504 of which were within exons (40.0% of DMLs). An additional 178
226 and 171 of the DMLs were found upstream and downstream of genes (within 2kb; 4.5% and
227 4.4%, respectively), and 188 were located within transposable elements (4.7%). There were 500
228 DMLs that were not found in any known feature (12.6%). 54% of DMLs had higher methylation
229 levels in SS (2,154 loci), and 46% were higher in HC (1,809) (Supplemental Figure 2).

230 Population divergence of methylation was also assessed at the gene level for gene
231 regions containing ≥ 5 informative loci. Of the 6,299 gene regions assessed, 1,447 were
232 differentially methylated (DMGs) as determined by binomial GLMs. DMGs and gene regions
233 containing DMLs were each enriched for 31 biological processes, both of which included
234 sarcomere organization (GO:0045214), and metabolic process (GO:0008152) (Supplemental
235 Table 2). Mean P_{ST} , a measure of population divergence in methylation (Johnson & Kelly 2020),
236 averaged across 14,088 random 10kb bins was $0.30 \pm SD 0.26$.

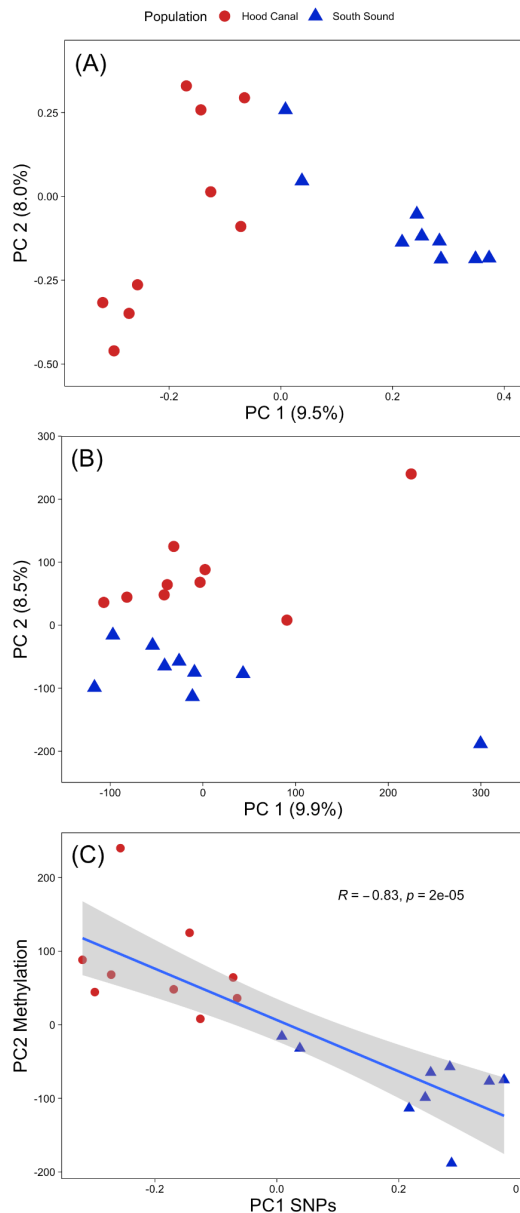


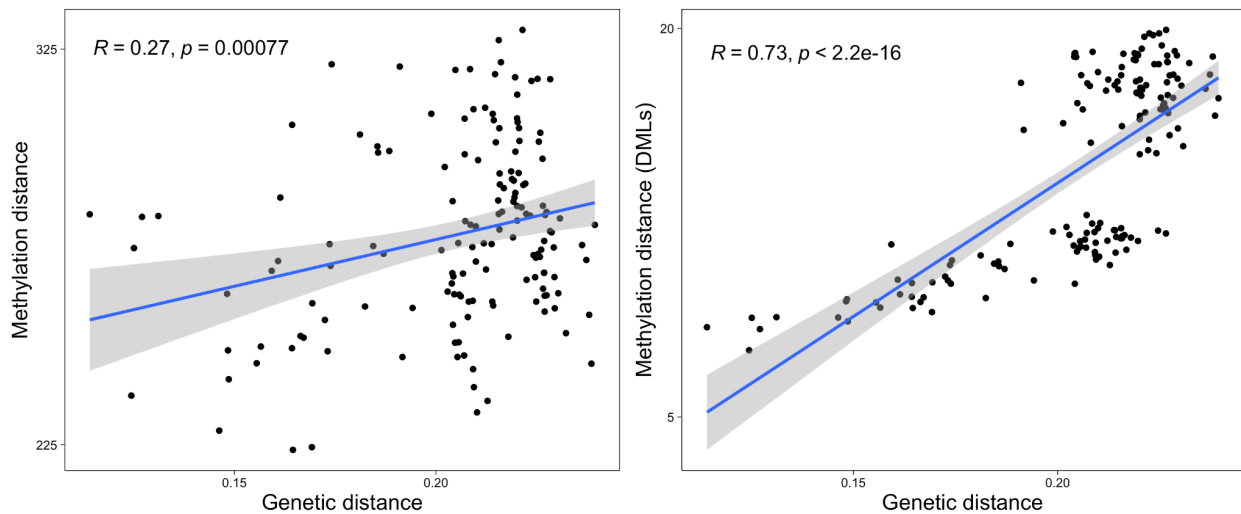
Figure 3: **A.** PCA of SNP data for the MBD18 samples. **B.** PCA of DNA methylation data (using all loci) for MBD18 samples. **C.** Scatter plot of PC1 from SNP genotype data and PC2 from DNA methylation data showing the linear regression line, Pearson correlation coefficient, and p-value.

237
238
239
240
241
242

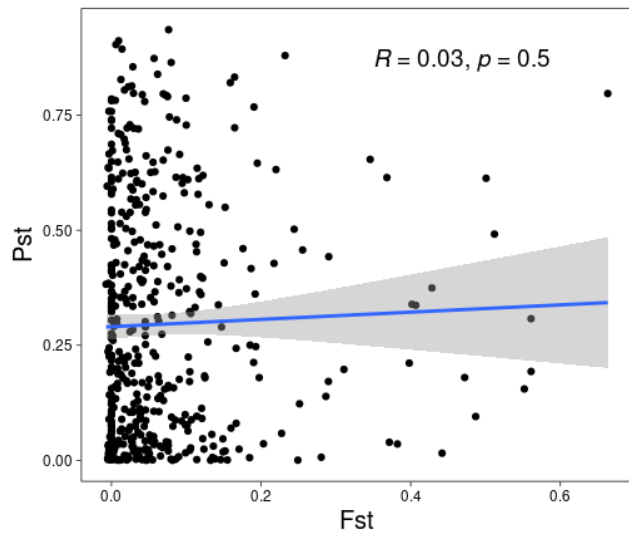
243 Relationship between genetic and epigenetic variation

244 To investigate the relationship between genetic and DNA methylation variation, we first
245 compared pairwise genetic distances between MBD18 samples with pairwise Manhattan
246 distance based on all filtered methylation data and found a weak, but significant relationship
247 (Pearson's $R = 0.27$, $p\text{-value} = 0.00077$ and Spearman's $\rho = 0.22$, $p\text{-value} = 0.0069$, Figure 4a).
248 This correlation was stronger when comparing against Manhattan distances based on DMLs

249 (Pearson's $R = 0.73$, p-value $< 2.2E10^{-16}$ and Spearman's $\rho = 0.70$ p-value $< 2.2E10^{-16}$) (Figure
 250 4b). This suggests that the rate of genetic changes between individuals is similar to the rate of
 251 methylation changes, especially for CpG sites that diverge between populations. We further
 252 compared population specificity of our data by correlating the 1st PC scores from SNP data
 253 (9.5% of variation, Figure 3a) with the 2nd PC scores of methylation data (8.5%, Figure 3b), as
 254 these two axes clearly separated individuals by population. These were strongly correlated
 255 (Pearson's $R = -0.83$, p-value = $1.65E10^{-5}$ and Spearman's $\rho = -0.86$, p-value $< 2.2E10^{-16}$,
 256 Figure 3c), suggesting that common underlying mechanisms may be involved in population
 257 divergence at variable genetic and epigenetic sites. However, we found no significant
 258 correlation between F_{ST} and P_{ST} at 827 random 10kb genomic bins where we had both SNP and
 259 methylation data (Figure 5). This result suggests that the strong correlation between population-
 260 specific genetic and epigenetic patterns on the individual level is not primarily driven by
 261 genomically linked epigenetic and genetic sites.



262 **Figure 4:** Epigenetic divergence as a linear function of genetic distance. The x axes represent genetic
 263 distances calculated from genotype probabilities for 5,269 SNPs. The y axes are the Manhattan distances
 264 from CpG methylation $\times 1000$ (a; using all methylation data and b; using DMLs). The linear regression
 265 lines are shown, together with the Pearson correlation coefficient and p-value.



266 **Figure 5:** Scatterplot of P_{ST} (measure of epigenetic divergence between populations) and F_{ST} (measure of
 267 genetic divergence) for 827 random 10kb genomic bins with both SNP and methylation data.

268 mQTL analysis

269 To determine if genetic variants are associated with loci showing inter-individual
 270 methylation variation, we conducted a mQTL analysis using a linear regression model in the R
 271 package MatrixEQTL (Shabaln 2012). For this analysis, we used 2,860 SNPs that had a MAF >
 272 0.05 across the MBD18 samples as the explanatory variable, PC1-3 of SNP genotype data as a
 273 covariate to control for ancestry, and the percent methylation at 232,567 CpG sites as the
 274 response variable. ‘Local’ mQTLs were determined to be SNPs within 50kb of the CpG and an
 275 un-adjusted p-value threshold of 0.01, while distant mQTLs were greater than 50kb from the
 276 CpG or on a different scaffold and had an FDR threshold of 0.05. Results of the mQTL analysis
 277 are summarized in Table 1, with 1,985 SNPs (69.4%) detected as mQTLs and 7,157 CpGs
 278 (3.1%) associated with a mQTL. Due to linkage disequilibrium (LD) among SNPs as well as our
 279 reduced representation genetic sequencing, most of these SNPs are unlikely to be the actual
 280 causal variant influencing the methylated site. Therefore, we follow the recommendation of

281 (McClay et al. 2015) and evaluate the methylated sites under genetic control as a better
282 representation of genetic influence on the methylome.

283 Compared to background rates, local mQTLs were overrepresented in gene regions (83
284 annotated genes, 67% vs. 37%, $p=8.665 \text{ E-}16$), as were their associated CpGs (78% vs. 59%,
285 $p=7.23\text{E-}9$) (Supplemental Figure 9). Genes containing these sites were functionally enriched
286 for the GO term “DNA repair” (8.7% of genes), InterPro term “SWI/SNF chromatin-remodeling
287 complex” (3.6%), and UP keywords “transcription regulation” (16.8%) and “disease mutation”
288 (18%), among other functions. Distant mQTL SNPs were found in 309 genes but were not
289 enriched for any functional categories. The CpG loci associated with distant mQTLs were found
290 in 1,809 annotated genes and enriched for the COG category “RNA processing and
291 modification” (0.7% of genes), 49 GO categories including “transcription DNA-templated”
292 (12.1%), “mRNA processing” (2.6%), “covalent chromatin modification” (2.4%), “regulation of
293 translational initiation” (0.66%), “chromatin remodeling” (1.1%), nucleic acid binding (5.7%),
294 chromatin binding (3.8%), and “transcription factor activity”(3.8%), as well as 87 UP keywords
295 and sequence features including “phosphoprotein”(49.7%), “nucleus” (33.2%), “acetylation”
296 (22%), “RNA-binding” (6.7%), “methylation” (6.4%), and “chromatin regulator” (3.9%). Some
297 genes containing these distantly controlled CpGs include 7 different RNA binding motif proteins,
298 6 RNA polymerase genes, 8 DEAD-box type helicases, 17 eukaryotic translation initiation factor
299 (eif) genes, and six SWI/SNF regulator of chromatin. While most other enrichment tests
300 presented here were not significant after Benjamini FDR correction ($P < 0.1$), 17 (10%) of the
301 enriched functions for CpGs with distant mQTLs were significant (Supplementary File 2).

302 SNPs that create or remove CpGs (CpG-SNPs) may contribute to individual differences
303 in methylation, and therefore lead to mQTL associations or correlations between genetic and
304 epigenetic distances. We identified 651 CpG-SNPs (12.4%) from our full set of 5,269 SNPs
305 through mapping to our draft genome. CpG-SNPs were more likely to be within 350bp of a

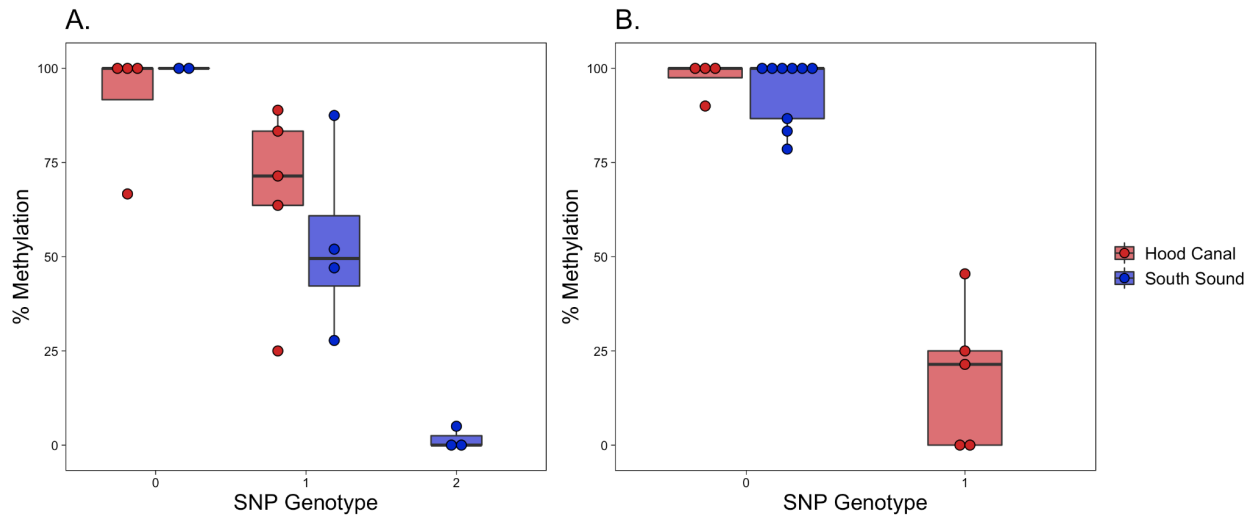
306 methylated CpG than non-CpG-SNPs (40.9% vs 34.5%, $p=0.00161$), when using all CpGs in
307 the genome as the background. This 350bp window size represents the maximum length of a
308 library fragment, and therefore is the maximum distance at which a CpG-SNP could directly
309 affect our measure of methylation. CpG-SNPs were slightly more likely to be within 350bp of a
310 DML than non-CpG-SNPs (0.9% vs 0.4%, $p=0.04086$), suggesting that CpG-SNPs only play a
311 minor role in creating DMLs. More of the methylated sites with local meth-QTLs had a CpG-SNP
312 compared to distant mQTLs (12 vs 8, $p=1.508e-13$). Due to the sparse genetic sequencing of
313 the genome, we are likely missing many CpG-SNPs associated with both local and distant
314 mQTLs.

315 We investigated the spatial overlap between population DMLs and CpGs associated with
316 local mQTLs, and found CpGs with local mQTLs were more likely to overlap with DMLs than
317 CpGs without an mQTL association (24.1% vs. 15.9%, $p=0.001289$). Genes of particular
318 interest included PRICKLE2 (developmental processes, linked to growth in *Crassostrea gigas*
319 (*Takeuchi et al. 2003; Yang et al. 2020*), TRIM2 (innate immunity, differential methylation to low
320 pH in *C. hongkongensis* larvae (*Ozato et al. 2008; Lim et al. 2020*)), eukaryotic translation
321 initiation factor 3 (eif3) (translation initiation through mRNA recruitment and interactions with
322 methyltransferases, response to low pH in *Saccostrea glomerata* (*Wolf et al. 2020; Ertl et al.*
323 *2016*), OXCT1 (ketone catabolic process, variably methylated in humans (*Feng et al. 2021*)),
324 Mapk6 (signal transduction, immune signaling in *S. glomerata* (*Ertl et al. 2016*)), and MLH3
325 (DNA mismatch repair protein (*Lipkin et al. 2000*)). Examples of two local mQTLs that are also a
326 DML are shown in Figure 6. A significantly lower proportion of distant mQTLs were associated
327 with DMLs (9.5%, $p = 1.243e-8$). Of these 655 sites, 363 were in 311 genes, which were
328 enriched for numerous processes relative to all distant mQTL genes, including functions related
329 to development, immune response, transcription factor activity, and coiled coil domains. Unlike

330 local mQTLs, distant mQTLs were deficient in DMLs relative to non-distant mQTLs (9.5% vs
 331 14%, $p < 2.2 \times 10^{-16}$).

332 **Table 1.** Summary statistics for mQTL analyses.

	Local (< 50kb) p < 0.01	Distant (> 50kb, different scaffolds) FDR < 0.05
Number of CpG loci tested	10,320	232,567
Number of SNPs tested	853	2,860
Number and percent of unique SNPs with mQTLs	181 (21.2%)	1,936 (67.7%)
Number and percent of unique methylated sites with mQTLs	240 (2.3%)	6,926 (3.0%)
Number and percent of methylated sites associated with an mQTL and a CpG-SNP / Number of tested sites with a CpG-SNP	12/179 (6.7%)	8/273 (2.9%)
Number and percent of methylated sites with an mQTL and a DML	58/240 (24.1%)	655/6926 (9.5%)



333 **Figure 6:** Two example CpG loci that are associated with a local SNP and are differentially
 334 methylated between populations. Each dot is an individual, with the genotype of the SNP on the
 335 x-axis and percent methylation on the y-axis. Boxplots are grouped and colored by population.
 336 A) CpG (Contig54624.19738) is found on a gene annotated as “similar to eif3d”, is differentially
 337 methylated 38.6% between populations, and associated with SNP Contig54624.19920. B) CpG
 338 (Contig60108.5780) is found on a gene annotated as “similar to MLH3”, is differentially
 339 methylated 37.3% between populations, and is associated with SNP Contig60108.2787.

340 Discussion

341 Research primarily from humans and plants have shown that both environment and
 342 ancestry can influence variation in DNA methylation, however these associations are still not
 343 fully understood in less studied taxa such as marine invertebrates. In this study, we describe the
 344 genotype x epigenotype relationship by integrating high-throughput genomic and methylation
 345 data for two distinct oyster populations raised in the same environment for one generation. In
 346 addition to providing the first characterization of genome-wide methylation patterns in the oyster
 347 genus *Ostrea*, our results show a clear association between genetic and epigenetic patterns of

346 variation. Underlying this association are both direct genetic changes in CpGs (CpG-SNPs), and
347 mQTLs with indirect functional influence on methylation. The association between genetic and
348 epigenetic patterns breaks down when comparing measures of population divergence at
349 specific genomic regions, suggesting that individual variation can outweigh population-level
350 variation when comparing these patterns at local genomic scales.

351 General DNA methylation patterns

352 *O. lurida* CpG methylation is disproportionately found in gene bodies. When compared to
353 all CpG loci in the genome, *O. lurida* methylation is ~3.7x more likely to occur in exons, and
354 ~1.4x more likely to occur in introns (Figure 1, Supplemental Figure 2). Gene body methylation
355 has also been reported for the Eastern oyster (*Crassostrea virginica*) (Venkataraman et al.
356 2020; Johnson & Kelly 2020; Downey-Wall et al. 2020), Pacific oyster (*C. gigas*) (Gavery &
357 Roberts 2013; Song et al. 2017; Wang et al. 2020, 2014), Hong Kong oyster (*C.*
358 *hongkongensis*) (Lim et al. 2020), and pearl oyster (*Pinctada fucata martensii*) (Zhang et al.
359 2020). The precise role and function of gene body methylation is not yet clear. However, in
360 contrast to the suppressive role of promoter methylation in vertebrates, gene body methylation
361 in invertebrates is hypothesized to mediate transcriptional activity because it is positively
362 associated with gene expression (Roberts & Gavery 2012). Without expression data we cannot
363 directly assess the relationship between genic methylation and transcription in *O. lurida*.
364 However the high preponderance for methylation in *O. lurida* exons, and to a lesser extent
365 introns, supports a role in mediating alternative splicing activity. That methylated genes in the *O.*
366 *lurida* genome are enriched for a variety of biological processes, including those related to cell
367 cycle and biogenesis, DNA, RNA and protein metabolism, transport, and stress response
368 (Supplemental Table 1), supports the theory that methylation regulates both housekeeping and
369 inducible processes in marine invertebrates.

370 Epigenetic and genetic population structure

371 Population-specific methylation patterns

372 Global DNA methylation patterns in *O. lurida* are influenced by population of origin
373 (Figure 3b), despite rearing oysters in common conditions. To examine biological functions
374 associated with differential methylation among these populations, we performed enrichment
375 analyses on both the 1,447 differentially methylated gene regions (DMGs) and genes containing
376 the 3,963 differentially methylated loci (DMLs) (Supplemental Table 2). DMGs and genes
377 containing DMLs were both enriched for biological processes involved in transport, cell
378 adhesion and migration, protein ubiquitination, and sarcomere organization. DMGs were also
379 enriched for 27 other processes, including several related to reproduction (e.g. germ cell
380 development, lipid storage, oogenesis), and growth (e.g. cell morphogenesis, epithelium
381 development, regulation of neurogenesis and growth). The two focal populations have distinct
382 abiotic stress tolerances, as well as reproductive and growth strategies, some of which have
383 been shown to be transgenerational (Silliman et al. 2018; Spencer et al. 2020; Heare et al.
384 2017). As gene expression is associated with methylation status in oysters (Gavery & Roberts
385 2013; Johnson et al. 2020), protein-coding genes identified here with population-specific
386 methylation rates are good candidates for future studies exploring epigenetic control of
387 phenotype in marine invertebrates.

388 Our methylation data is biased towards hyper-methylated loci (average proportion
389 methylation for loci with 5x coverage is ~80%, and only 2.5% of sequenced loci had no
390 methylated reads)(Supplemental Figure 1). This type of data is excellent for characterizing the
391 methylation landscape, but does limit our ability to compare loci where methylation varies
392 significantly among populations (e.g. loci that are hyper-methylated in one population, but hypo-
393 methylated in the other). To partially mitigate this concern, we implemented a filtering approach

394 that is atypical of MBD-BS studies in order to include some such divergently methylated loci that
395 may be missed with otherwise strict data filtering. Of these 251 included loci, 246 were DMLs
396 and 17 were associated with distant mQTLs, supporting this choice when going forward with
397 comparative MBDseq or MBD-BS. As the cost of sequencing decreases, other sequencing
398 methods (e.g. WGBS) should be used to detect other regions where methylation differs
399 substantially. However, by detecting population-specific epigenetic differences, our results
400 contribute to the limited number of studies from *Crassostrea* oyster species that also found
401 population-specific (Johnson & Kelly 2020; Zhang et al. 2018) or family-specific methylation
402 patterns (Olson & Roberts 2014). In contrast to these previous studies, the present study
403 controls for changes to the methylome that could arise due to differing environments during
404 development. Therefore, the observed population-specific methylation patterns reflect either
405 heritable methylation differences, or those acquired as germ cells in the parental environments.

406 Population genetic variation

407 Low but significant population genetic divergence had previously been described for
408 Olympia oyster populations in Puget Sound using de novo genotype-by-sequencing and 2b-
409 RAD data (Silliman et al. 2018; Silliman 2019). The current study validates these findings using
410 a reference-based 2b-RAD approach and 5,269 SNPs, finding weak ($F_{ST} = 0.059$), but significant
411 genetic differentiation (Figure 2, Supplemental Figure 7). Similar genetic differentiation patterns
412 are observed for other bivalve species on comparable spatial scales, such as the Eastern oyster
413 (*C. virginica*) and the Pacific oyster (*C. gigas*) (Johnson & Kelly 2020; Kawamura et al. 2017).
414 Given the potential for gene flow between neighboring oyster populations during the planktonic
415 larval stage, the continued evidence for population genetic differentiation suggests that either
416 larvae do not disperse as far as would be predicted (Shanks 2009; Pritchard et al. 2015), or that

417 adaptive and neutral processes can override the effects of gene flow for some parts of the
418 genome (Sanford & Kelly 2011; Weersing & Toonen 2009).

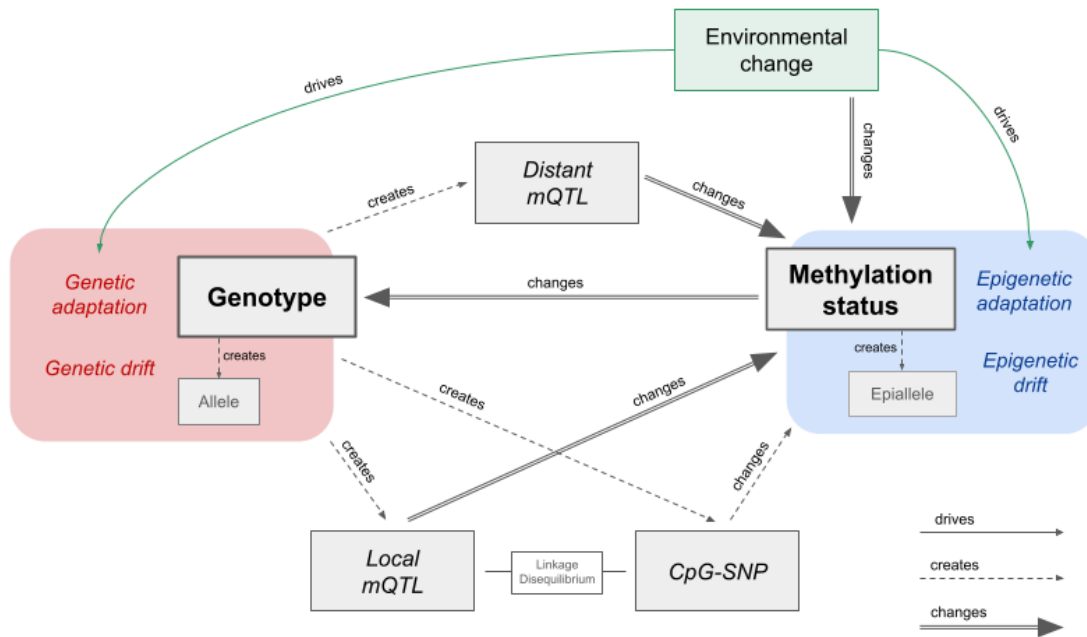
419 A benefit of using a reference genome in this study is the ability to also evaluate
420 functional patterns of genetic divergence. SNPs in genes had lower mean F_{ST} than the genome-
421 wide average, which aligns with expectations of gene bodies in general showing higher
422 sequence conservation due to purifying selection (Kimura 1983). Two gene regions contained
423 outlier SNPs, and therefore may be under divergent selection: G2/mitotic-specific cyclin-B and
424 SOCS5. G2/mitotic-specific cyclin-B is associated with gametogenesis in *C. gigas* (Dheilly et al.
425 2012), as well as tidally-influenced gene expression changes in the mussel *Mytilus californianus*
426 (Gracey et al. 2008). SOCS5, a member of the cytokine signaling family, is highly expressed in
427 hemocytes, gills, and the digestive gland of *C. gigas* (Li et al. 2015). Our 2b-RAD SNPs only
428 represented 1,386 genes out of 32,211 in the genome, and therefore our outliers are likely only
429 a fraction of genes diverging between these populations (Lowry et al. 2017). Nevertheless,
430 these genes should be added to a growing list of candidate loci to investigate further for local
431 adaptation in the Olympia oyster (Silliman 2019; Heare et al. 2018; Maynard et al. 2018).

432 Associations between methylation patterns and genetic variation

433 Previous studies associating genetic variation and DNA methylation patterns in marine
434 invertebrates mainly compared measures of population divergence (e.g., F_{ST} and P_{ST}) at
435 overlapping genomic regions, and found little or no relationship (Johnson & Kelly 2020; Wang et
436 al. 2020; Liew et al. 2020). In the current study, we also found no relationship between F_{ST} and
437 P_{ST} for overlapping genomic regions. However, by further comparing genome-wide summary
438 statistics and PCAs at the individual level, we revealed the significant relationship between
439 interindividual patterns in methylation and genetic variation, with 27% of variation in inter-
440 individual methylation differences explained by genetic distance. Similar analyses have found

441 significant correlations in reef-building coral (Dimond & Roberts 2020) and humans (Carja et al.
442 2017). By only focusing on measures of population differentiation, previous marine invertebrate
443 studies may have missed couplings between methylation and genetic patterns. There are three
444 nonexclusive scenarios that could explain the observed relationship between genetic and
445 epigenetic patterns: 1) genetic state results in methylation change (e.g. CpG-SNPs), 2)
446 methylation state results in genetic change, and 3) epigenetic and genetic changes occur in
447 parallel due to independent molecular mechanisms, but are associated through either physical
448 linkage or shared evolutionary pressures (Figure 7).

449 CpG-SNPs have been implicated as important drivers of genome-epigenome
450 interactions in vertebrates, either by removing a CpG site on one or both strands and directly
451 disrupting methylation, or by influencing local methylation activity (Zhi et al. 2013; McClay et al.
452 2015). A considerable proportion of the SNPs in our study were CpG-SNPs (12.3%), 40.1% of
453 which were within 350bp of a methylated CpG, and therefore capable of influencing our MBD-
454 BS measurements. The enrichment of CpG-SNPs associated with methylated CpGs supports
455 the hypothesis that methylation could have preceded and induced genetic variation by altering
456 genome stability and mutation rates (Flores et al. 2013). Methylated cytosines readily mutate to
457 thymine by deamination, which results in an overall depletion of CpG dinucleotides (Coulondre
458 et al. 1978; Schorderet & Gartler 1992; Bird 1980). For instance, in the Pacific oyster *C. gigas*
459 mutation rate is biased towards GC → AT, particularly at methylated CpG sites, and in coding
460 regions (Song 2020), and genes predicted to have low levels of methylation (analyzed in-silico
461 using the established CpG observed / expected relationship) are less



462 **Figure 7:** Molecular and evolutionary mechanisms linking genetic variation and methylation variation.
 463 DNA mutations can change or create methylation epialleles at CpGs, either directly through CpG-SNPs,
 464 or indirectly through the creation of local or distant mQTLs. Some of these mQTL associations will be
 465 spurious, due to linkage disequilibrium (LD) with CpG-SNPs or other mQTLs. Methylation epialleles can
 466 be created or changed by stochastic epimutations or external signals from the environment. Methylation
 467 status in turn can change the rate of DNA mutations at a local scale. Observed epigenetic and genetic
 468 associations may instead be due to independent molecular mechanisms that occur in parallel due to
 469 shared evolutionary pressures.

470 genetically diverse (analyzed via SNPs) (Roberts & Gavery 2012). Alternatively, some CpG-
 471 SNPs may have preceded methylation and led to beneficial methylation variation, in which case
 472 they may be associated with mQTLs.

473 High-density methylome and genotyping studies in model taxa have determined that a
 474 substantial proportion of variably methylated sites are under local genetic control by mQTLs. To
 475 our knowledge, this is the first mQTL analysis in a marine invertebrate. We found 7,166 of

476 tested CpGs were under genetic control, either locally (2.3%) or distantly (3.0%). This is lower
477 than that found for human blood cells (15% local, 0.08% distant)(McClay et al. 2015) and
478 *Arabidopsis thaliana* (18%) (Dubin et al. 2015), although our study has much lower coverage in
479 both methylation and genetic data. The McClay human study also found that 97.7% of SNPs
480 were local meth-QTLs, which is much higher than the 21% found in our study. One likely
481 explanation for this is the highly fragmented status of our draft genome, with 158,535 scaffolds
482 under 50kb in length. It is likely that some SNPs within 50kb of a CpG were actually tested as
483 distant mQTLs. While our mQTL analysis is not entirely comparable to larger scaled studies in
484 humans and plants, it nevertheless shows that associations with genetic variants can be a
485 significant source of variation in methylation, and should therefore be investigated further with
486 whole genome genotyping. CpG-SNPs are one possible mechanism underlying local mQTLs,
487 and we do see an enrichment of CpG-SNPs in local mQTLs compared to distant mQTLs. This
488 result has also been seen in model organisms and humans, however in those cases CpG-SNPs
489 contributed to over 75% of local mQTLs (McClay et al. 2015).

490 For mQTLs that lack CpG-SNPs, alternative mechanisms must be considered. Binding
491 of transcription factors has been linked to changes in local methylation levels, for example a
492 loss of methylation upon transcription factor binding (Héberlé & Bardet 2019). In this framework,
493 a SNP within a transcription factor binding site may affect methylation locally, while a SNPs that
494 affects the expression or activity of transcription factors could generate changes in methylation
495 wherever the transcription factor binds (Lienert et al. 2011; Martin-Trujillo et al. 2020). Our
496 functional enrichment tests suggest this mechanism may be acting in *O. lurida* by finding genes
497 with mQTL SNPs enriched for “DNA-binding” and “transcription regulation”, and five distant
498 mQTLs SNPs within genes involved in transcription factor complexes. Genetic differences that
499 affect binding of different chromatin classes have also been shown to modulate local
500 methylation patterns (Jeffery & Nakielny 2004; Banovich et al. 2014). One particularly exciting

501 result is that genes containing distantly associated CpGs were highly enriched for RNA
502 processing and binding functions, including multiple RNA binding motif proteins and DEAD-box
503 RNA helicases. DEAD-box RNA helicases are known to co-regulate transcription factors and
504 contribute to chromatin remodeling in multicellular organisms, although the exact molecular
505 mechanisms are still unclear (Giraud et al. 2018). They have also been linked to epigenetic
506 control of abiotic stress-responsive transcription factors in plants through an RNA-directed DNA
507 methylation pathway (Barak et al. 2014). More research integrating chromatin annotations (e.g.,
508 ATACseq), CpG methylation, genetic diversity, and gene expression are required to begin
509 elucidating how these mechanisms interact to drive phenotypic divergence.

510 To confidently state that epigenomic variation is under genetic control for all detected
511 local mQTLs, one assumes that epigenetic inheritance by other means is absent. If epigenetic
512 marks can be inherited between generations, then associations with local genetic variants may
513 simply be due to LD between the segregating epiallele and nearby SNPs. Epigenetic inheritance
514 is well characterized in plants (Taudt et al. 2016), and there is evidence of environmentally-
515 driven epigenetic changes that persist across generations in corals and oysters, although the
516 mechanisms of invertebrate epigenetic inheritance is still not understood (Johnson et al. 2020;
517 Downey-Wall et al. 2020; Lim et al. 2020; Wang et al. 2020; Akcha et al. 2020; Venkataraman et
518 al. 2020). It is also possible that genetic variants and epialleles may be under parallel selection
519 due to phenotype-genotype interactions, which may lead to a spurious mQTL association
520 (Schmid et al. 2018; Taudt et al. 2016). However, since epialleles can undergo both forward and
521 backward changes, epimutation rates are much higher than DNA mutations and therefore
522 spurious mQTL associations will break down rapidly. Comparing mQTL analyses between
523 generations would help identify both the heritability of CpG methylation and the consistency of
524 mQTL results.

525 Evolutionary implications

526 Many marine invertebrates with large ranges experience spatial heterogeneity in abiotic
527 and biotic factors that lead to population-level divergence in fitness-related traits (Sanford &
528 Kelly 2011). This environmentally-driven divergence may be facilitated through phenotypic
529 plasticity, selection for locally-favorable genotypes, or a combination. Here we were able to
530 examine the primary molecular mechanisms underlying plasticity and adaptation: epigenetic
531 modifications and genetic variation. Interestingly, in this system we found a clear coupling of the
532 two, with 27% of individual epigenetic variation attributable to genetics. This result has profound
533 implications for studies of both evolutionary processes and molecular machinery. First, studies
534 of plasticity and epigenetic variation among groups from different environments must also
535 account for genetic variation, rather than attributing all differences to the environment. Second,
536 as genetic variation is clearly heritable, our results suggest that some proportion of DNA
537 methylation (and likely associated phenotypes) are also heritable. Finally, despite our two
538 populations being raised in the same environment, 73% of the epigenetic variation in our system
539 was not attributable to genetics. Characterizing the basis of this additional epigenetic diversity,
540 such as a historical influence of the environment or independent heritable mechanisms, will
541 identify avenues adjacent to genetic adaptation for producing long-term shifts in phenotype.

542 Methods

543 Draft Genome Assembly and Annotation

544 To facilitate the analysis of genetic and epigenetic data, a draft genome for the Olympia
545 oyster was developed using a combination of short-read sequence data (Illumina HiSeq4000)
546 combined with long-read sequence data (PacBio RSII) using PBJelly (PBSuite_15.8.24; English

547 et al, 2012). Short reads (NCBI SRA: SRP072461) were assembled using SOAPdenovo (Li et
548 al, 2008). The scaffolds (n=765,755) from this assembly were combined with the PacBio long-
549 read data (NCBI SRA: SRR5809355) using PBJelly (PBSuite_15.8.24; English et al, 2012).
550 Assembly with PBJelly was performed using the default settings. Only contigs longer than 1000
551 bp were used for further analysis. Genome assembly parameters were compiled using QUAST
552 (v4.5; Gurevich et al, 2013).

553 Genome annotation was performed using MAKER (v.2.31.10; Campbell et al, 2014)
554 configured to use Message Passing Interface (MPI). A custom repeat library for use in MAKER
555 was generated using RepeatModeler (open-1.0.11; . Hubley and Smit, 2008). RepeatModeler
556 was configured with the following software: RepeatMasker (open-4.0.7; configured with
557 Repbase RepeatMasker v20170127; (Bao et al. 2015), RECON (v1.08; Bao and Eddy, 2002)
558 with RepeatMasker patch, RepeatScout (v1.0.5; Price et al, 2005) and RepeatMaskerBlast
559 (RMBLast (2.6.0)) configured with the isb-2.6.0+-changes-vers2 patch file, and TRF (v4.0.4;
560 Benson, 1999).

561 MAKER was run on two high performance computing (HPC) nodes (Lenov NextScale,
562 E5-2680 v4 dual CPUs, 28 cores, 128GB RAM) on the University of Washington's shared
563 scalable compute cluster (Hyak) using the icc_19-ompi_3.1.2 module (Intel C compiler v19,
564 Open MPI v3.1.2). An Olympia oyster transcriptome assembly was used for EST data. Protein
565 data used was a concatenation of NCBI proteomes from *Crassostrea gigas* and *Crassostrea*
566 *virginica*. *Ab-initio* gene training was performed twice using the included SNAP software (Korf,
567 2004). Functional protein annotation was performed using BLASTp (v.2.6.0+; Altschul et al,
568 1990) against a UniProt SwissProt BLAST database (FastA file formatted using BLAST 2.8.1+)
569 downloaded on 01/09/2019. The MAKER functions `maker_functional_gff` and
570 `maker_functional_fasta` both used the same UniProt SwissProt BLAST database. Protein
571 domain annotation was performed using InterProScan 5 (v5.31-70.0; Jones et al, 2014). Code

571 and data files used for genome annotation are available in the accompanying repository
572 <https://github.com/sr320/paper-oly-mbdbbs-gen>.

573 Experimental Design

574 DNA was extracted from adductor muscle tissue from 184 individuals (88 from Hood
575 Canal and 96 from Oyster Bay), using E.Z.N.A. Mollusc Kit with RNase A treatment (Omega)
576 according to the manufacturer's instructions. DNA quality was examined on a 1% TAE agarose
577 gel and DNA concentration was determined using the dsDNA BR Assay Kit on a Qubit 2
578 fluorometer (Invitrogen).

579 Genetic Analysis

580 2bRAD Sequencing and Genotyping

581 Using a 2b-RAD reduced-representation sequencing approach (Wang et al. 2012), we
582 sequenced 184 individuals and 53 technical replicates from the two Puget Sound populations
583 for a total of 237 samples across 4 lanes of 50bp single-end Illumina HiSeq2500 and 1
584 HiSeq4000 lane. The frequent-cutter restriction enzyme Alfl was used with modified adaptors
585 (5'-NNR-3') to target $\frac{1}{4}$ of all Alfl restriction sites in the genome. We followed the 2bRAD library
586 protocol developed by Eli Meyer (available at <https://github.com/sr320/paper-oly-mbdbbs-gen>),
587 except that we used 900 ng of starting DNA, 19 PCR cycles as determined by a test PCR, and
588 we concentrated the final pooled libraries using a Qiagen PCR kit prior to sequencing.
589 Sequencing and sample demultiplexing was performed by GENEWIZ for the four HiSeq2500
590 lanes and the University of Chicago's Functional Genomics Center for the one HiSeq4000 lane.
591 Sequencing of some of these samples was previously described in (Silliman et al. 2018).

592 Scripts by Mikhail Matz were used for quality filtering, read trimming, and mapping to
593 the reference genome (https://github.com/z0on/2bRAD_denovo). Read trimming was performed
594 by cutadapt (Martin 2011). Samples were retained for mapping to the genome and genotyping if
595 they had greater than 1.3 million reads after filtering. Samples were mapped to the genome
596 using Bowtie2 with the --local option (Langmead & Salzberg 2012). Genotype likelihoods were
597 calculated using ANGSD (Korneliussen et al. 2014) with the following filters: no triallelic sites, p-
598 value that SNP is true $1e-3$, minimal mapping quality 20, minimal base quality 25, minimal
599 number of genotyped individuals 80 (~70% of individuals passing filter), minimal number of
600 reads at a site 3, minimum p-value for strand bias $1e-5$, and minimum overall allele frequency
601 0.01. This filtering retained 114 samples and 5,269 SNPs.

602 Genetic distance, PCA, Admixture

603 The genotype likelihoods produced by ANGSD were used for examining population
604 genetic structure and estimating pairwise genetic distance. NGSadmix was used to perform an
605 ADMIXTURE analysis based on genotype likelihoods of 3,724 SNPs, after filtering further for a
606 minimum overall allele frequency of 0.05 (Skotte et al. 2013). The most likely number of genetic
607 clusters (K) was determined using the (Evanno et al. 2005) method by running NGSadmix 10
608 times for each value of K, with K ranging from one to five, and then uploading the results to
609 Clumpak (Kopelman et al. 2015). The q values for the best K were plotted in R. Pairwise genetic
610 distances between all individuals were estimated using ngsDist with default parameters (Vieira
611 et al. 2016). A matrix of genetic distances for the MBD18 samples was subsetted and used for
612 comparative analyses with methylation data.

613 For a Principal Components Analysis (PCA) of all samples, we used ANGSD to estimate
614 a covariance matrix by sampling a single read at each polymorphic site using the same filtering
615 parameters as previously described. We then performed an eigenvalue decomposition on the

616 matrix and plotted the PCA in R. For the PCA on only the MBD18 samples, we subsetted the
617 covariance matrix and ran an eigenvalue decomposition on those samples alone.

618 To detect SNPs under putative directional selection, we used qctool v2.0
619 (https://www.well.ox.ac.uk/~gav/qctool_v2/) to convert our genotype likelihoods to a VCF of
620 SNPs with > 90% confidence. SNPs with less than 90% confidence were coded as missing. We
621 used BayeScan v2.1 (Foll & Gaggiotti 2008) with 1:10 prior odds, 100,000 iterations, a burn-in
622 length of 50,000, a false discovery rate (FDR) of 10%, and default parameters. Results were
623 visualized in R.

624 To measure population genetic differentiation (F_{ST}), we used the realSFS command in
625 ANGSD to estimate the Site Frequency Spectrum (SFS) separately for each population, then
626 calculated the 2D-SFS which was used as a prior for estimating the joint allele frequency
627 probabilities at each site. In order to avoid distorting the allele frequency spectrum, we did not
628 filter our data based on the p-value that a SNP was true or for minimum allele frequency. We
629 then filtered out potential lumped paralogs sites by removing sites where heterozygotes likely
630 compromised more than 75% of all genotypes. This filtering strategy resulted in 363,405 sites
631 and 5,882 SNPs. Global F_{ST} between populations and per-site F_{ST} was calculated using
632 ANGSD, based on (Reynolds et al. 1983). A weighted F_{ST} estimate was calculated for each
633 gene by including all SNPs within \pm 2kb of an annotated gene region.

634 DNA Methylation

635 MBD-BS Library Preparation and Alignment

636 DNA was isolated from adductor tissue using the E.Z.N.A. Mollusc Kit (Omega)
637 according to the manufacturer's protocol. A total of 18 samples were extracted for DNA
638 methylation analysis, 9 from the Hood Canal population and 9 from the Oyster Bay population.
639 Samples were sheared to a target size of 350bp using a Bioruptor 300 (Diagenode) sonicator.

640 Fragmentation was confirmed with a Bioanalyzer 2100 (Agilent). Methylated DNA was selected
641 using the MethylMiner Methylated DNA Enrichment Kit (Invitrogen) according to the
642 manufacturer's instructions for a single, high-salt elution. Samples were sent to ZymoResearch
643 for bisulfite conversion, and Illumina library preparation for 50bp single-end reads and
644 sequencing with the Pico Methyl-Seq Library Prep Kit (ZymoResearch). Samples were
645 multiplexed into a single library and sequenced on an Illumina HiSeq2500 (Illumina). This library
646 was sequenced across three lanes to achieve the desired number of reads.

647 Sequence quality was checked by FastQC v0.11.8 and adapters were trimmed using
648 TrimGalore! version 0.4.5 (Andrews 2010; Krueger 2012). Bisulfite-converted genomes were
649 created in-silico with Bowtie 2-2.3.4 (Linux x84_64 version; (Langmead & Salzberg 2012) using
650 bismark_genome_preparation through Bismark v0.21.0 (Krueger & Andrews 2011). Trimmed
651 reads were aligned to these genomes with Bismark v0.21.0. Alignment files were deduplicated
652 with deduplicate_bismark and sorted using SAMtools v.1.9 (Li et al. 2009). Methylation calls
653 were extracted from sorted deduplicated alignment files using coverage2cystosine with --
654 merge_CpG parameter.

655 General DNA methylation landscape

656 To assess general methylation patterns in *O. lurida*, quality trimmed MBD-BS reads from
657 all samples (n=18) were concatenated, then re-aligned to the genome using Bismark with
658 settings as described above. Only loci with at least 5x coverage were examined. A cytosine
659 locus was deemed methylated if 50% or more of the reads remained cytosines after bisulfite
660 conversion (Gavery & Roberts 2013; Venkataraman et al. 2020). To characterize methylation
661 landscape, loci were intersected with the following *O. lurida* genome features using bedtools
662 v2.29.0: exons, introns, gene flanking regions (2kb upstream and downstream), transposable
663 elements, and unknown regions (Quinlan 2014). All CpG loci in the *O. lurida* draft genome were

664 similarly annotated to characterize the distribution of candidate CpG methylation sites across
665 features. Using chi-squared contingency tests in R, we examined whether the distribution of
666 methylated loci across genomic features differed from the distribution of all CpG sites in the
667 genome ($\alpha=0.05$).

668 Comparative methylation analyses

669 Associations between *O. lurida* population (Hood Canal, South Puget Sound) and
670 methylation patterns were examined by assessing differentially methylated loci (DMLs) and
671 differentially methylated gene regions (DMGs). Bismark alignment files (.bam format) were first
672 processed in methylKit (version 1.8.1) (Akalin et al. 2012) by using processBismarkALn to
673 convert them to a methylRawList object, which contains per-base methylation calls for each
674 sample. Loci were filtered to retain those with at minimum 5x coverage using
675 filterByCoverage, and unite selected only loci that were retained across 7 of the 9
676 samples within each population (N=18). Additional loci were included in the comparative
677 analyses to incorporate loci that were very likely unmethylated in one population but highly
678 methylated in the other, which is not captured in MBDSeq data due to the heavy bias for
679 methylated regions. This was accomplished by identifying CpG loci that were widely sequenced
680 in one population (data present for seven of the nine samples) and minimally sequenced in the
681 other population (data present for one sample or less), and assuming that the samples with no
682 data in the low-sequenced population were unmethylated at 5x coverage. Global differences in
683 methylation patterns were assessed by Principal Component Analysis (PCA) using the
684 PCASamples function (a version of prcomp), from a percent methylation matrix that was built
685 using perCMethylation. A matrix of sample x sample manhattan distances was generated
686 from the percent methylation matrix using dist() from the stats package for R v4.0.4 and used for
687 comparative analyses with genetic data.

688 Differentially Methylated Loci (DMLs)

689 DMLs were determined for each CpG locus using logistic regression in MethylKit with
690 `calculateDiffMeth`, and P-values were adjusted to Q-values using the SLIM method (Wang
691 et al. 2011). Loci with Q-value < 0.01 and percent methylation difference > 25% were determined
692 to be differentially methylated (DMLs).

693 Differentially Methylated Gene Regions (DMGs)

694 Gene regions were assessed for differential methylation among populations. Methylated
695 loci that overlapped with known gene regions were identified using the BEDtools
696 `intersectBed` function, a list of known genes that were identified using the genome
697 annotation tool MAKER (Cantarel et al. 2008), and expanded to include 2kb upstream and
698 downstream of gene bodies using BEDtools `slopBed`. Gene regions were assessed
699 individually for differential methylation between oyster populations using binomial GLMs and
700 Chi-square tests (Liew et al. 2018). P-values were adjusted using the Benjamini and Hochberg
701 method (Benjamini & Hochberg 1995). Gene regions that contained fewer than 5 methylated
702 loci were discarded prior to GLM analysis. Epigenetic divergence was estimated by P_{ST}
703 (Johnson & Kelly 2020) for 14,088 random 10kb bins using `Pst` from the `Pstat` R package
704 (Blondeau Da Silva Stephane [aut 2017]).

705 Gene Enrichment Analyses

706 DMGs and genes that contain DMLs were each tested for enriched biological functions.
707 For each gene set, gene sequences were merged with the *O. lurida* genome to generate a list of
708 Uniprot IDs from annotated genes. Enriched biological processes in each gene set were
709 identified with the Gene-Enrichment and Functional Annotation Tool from DAVID v6.8 as those
710 with modified Fisher Exact P-Values (EASE Scores) < 0.1 (Huang et al. 2009).

711 Comparing DNA Methylation and Genetics

712 To investigate the relationship between genetic and DNA methylation variation, we
713 compared summary statistics at both the level of the individual and genomic region for the 18
714 individuals where we had both genetic and epigenetic data (MBD18). First we compared
715 pairwise genetic distances based on 5,269 SNPs against pairwise Manhattan distances based
716 on all filtered methylation data, and determined both the Pearson and Spearman correlations in
717 R. We also compared the distances when only using DMLs for methylation distances (Figure 4).
718 We then assessed the correlation between the 1st PC scores from SNP data against the 2nd
719 PC scores of methylation data (Figure 3). We also calculated mean F_{ST} and P_{ST} for the 827
720 10kb genomic bins where we had both SNP and methylation data. These F_{ST} and P_{ST} values
721 were calculated as previously described for gene regions, with overlapping 10kb regions
722 identified with BEDtools (Quinlan 2014). To identify CpG-SNPs in our set of 5,269 SNPs, we
723 used the `injectSNPsMAF` and `getCpGsetCG` functions in the R package `RaMWAS` v1.18
724 (Shabalín et al. 2018) and the package `bedR` v1.0.7 (Haider et al. 2016).

725 To determine the relationship between regions of the genome with genetic variation and
726 regions with inter-individual methylation variation, we conducted a mQTL analysis using a linear
727 regression model 'modelLINEAR' in the R package `MatrixEQTL` (Shabalín 2012). CpGs were
728 removed if no samples had greater than 12% difference in methylation, resulting in 232,567
729 CpGs for the analysis. Methylation values were corrected using the inverse quantile normal
730 transformation of ranked values using custom R code (McCaw et al. 2020). 2,860 SNPs
731 remained after filtering for those genotyped in at least 7 individuals of both populations and with
732 an overall MAF > 0.05. To control for ancestry, the first three PCs of the SNP data were
733 included as covariates in the regression model. Local mQTLs were determined to be SNPs
734 within 50kb of the CpG and a p-value threshold of 0.01, while distant mQTLs were greater than
735 50kb from the CpG or on a different scaffold, had a p-value threshold of 0.01, and an FDR of

736 1% after Benjamini–Hochberg correction. Summary and plotting of mQTL loci was performed in
737 R and ggplot2 (Wickham 2016). Gene regions containing mQTL SNPs and their associated
738 CpGs were analyzed for functional enrichment with DAVID as described for DMLs, however for
739 the CpGs associated with distant mQTLs we used an EASE score cutoff of 0.05.

740 References

- 741 Akalin A et al. 2012. methylKit: a comprehensive R package for the analysis of genome-wide
742 DNA methylation profiles. *Genome Biol.* 13:R87.
- 743 Akcha F, Barranger A, Bachère E. 2020. Genotoxic and epigenetic effects of diuron in the
744 Pacific oyster: in vitro evidence of interaction between DNA damage and DNA methylation.
745 *Environ. Sci. Pollut. Res. Int.* doi: 10.1007/s11356-020-11021-6.
- 746 Andrews S. 2010. *FastQC*. <http://www.bioinformatics.babraham.ac.uk/projects/fastqc/>.
- 747 Banas NS et al. 2015. Patterns of River Influence and Connectivity Among Subbasins of Puget
748 Sound, with Application to Bacterial and Nutrient Loading. *Estuaries Coasts.* 38:735–753.
- 749 Banovich NE et al. 2014. Methylation QTLs are associated with coordinated changes in
750 transcription factor binding, histone modifications, and gene expression levels. *PLoS Genet.*
751 10:e1004663.
- 752 Bao W, Kojima KK, Kohany O. 2015. Repbase Update, a database of repetitive elements in
753 eukaryotic genomes. *Mob. DNA.* 6:11.
- 754 Barak S, Singh Yadav N, Khan A. 2014. DEAD-box RNA helicases and epigenetic control of
755 abiotic stress-responsive gene expression. *Plant Signal. Behav.* 9:e977729.
- 756 Bell O, Tiwari VK, Thomä NH, Schübeler D. 2011. Determinants and dynamics of genome
757 accessibility. *Nat. Rev. Genet.* 12:554–564.
- 758 Benjamini Y, Hochberg Y. 1995. Controlling the False Discovery Rate: A Practical and Powerful
759 Approach to Multiple Testing. *J. R. Stat. Soc. Series B Stat. Methodol.* 57:289–300.
- 760 Bird AP. 1980. DNA methylation and the frequency of CpG in animal DNA. *Nucleic Acids Res.*
761 <https://academic.oup.com/nar/article-abstract/8/7/1499/2359884>.
- 762 Blondeau Da Silva Stephane. 2017. Pstat-package: Assessing Pst Statistics in Pstat: Assessing
763 Pst Statistics. <https://rdr.io/cran/Pstat/man/Pstat-package.html> (Accessed March 23, 2020).
- 764 Bonder MJ et al. 2017. Disease variants alter transcription factor levels and methylation of their
765 binding sites. *Nat. Genet.* 49:131–138.
- 766 Cantarel BL et al. 2008. MAKER: an easy-to-use annotation pipeline designed for emerging
767 model organism genomes. *Genome Res.* 18:188–196.
- 768 Carja O et al. 2017. Worldwide patterns of human epigenetic variation. *Nat Ecol Evol.* 1:1577–
769 1583.
- 770 Chan F et al. 2017. Persistent spatial structuring of coastal ocean acidification in the California
771 Current System. *Scientific Reports.* 7:e2526.
- 772 Coulondre C, Miller JH, Farabaugh PJ, Gilbert W. 1978. Molecular basis of base substitution
773 hotspots in *Escherichia coli*. *Nature.* 274:775–780.

- 774 Danchin É et al. 2011. Beyond DNA: integrating inclusive inheritance into an extended theory of
775 evolution. *Nat. Rev. Genet.* 12:475–486.
- 776 Dheilly NM et al. 2012. Gametogenesis in the Pacific oyster *Crassostrea gigas*: a microarrays-
777 based analysis identifies sex and stage specific genes. *PLoS One.* 7:e36353.
- 778 Dimond JL, Roberts SB. 2020. Convergence of DNA Methylation Profiles of the Reef Coral
779 *Porites astreoides* in a Novel Environment. *Frontiers in Marine Science.* 6:792.
- 780 van Dongen J et al. 2016. Genetic and environmental influences interact with age and sex in
781 shaping the human methylome. *Nat. Commun.* 7:11115.
- 782 Downey-Wall A, Cameron L, Ford B, McNally E. 2020. Ocean acidification induces subtle shifts
783 in gene expression and DNA methylation in mantle tissue of the Eastern oyster (*Crassostrea*
784 *virginica*). *Front. Mar. Sci.* 7:566419.
- 785 Dubin MJ et al. 2015. DNA methylation in *Arabidopsis* has a genetic basis and shows evidence
786 of local adaptation. *Elife.* 4:e05255.
- 787 Eirin-Lopez JM, Putnam HM. 2019. Marine Environmental Epigenetics. *Ann. Rev. Mar. Sci.*
788 11:335–368.
- 789 Ertl NG, O'Connor WA, Wiegand AN, Elizur A. 2016. Molecular analysis of the Sydney rock
790 oyster (*Saccostrea glomerata*) CO₂ stress response. *Climate Change Responses.* 3:1–19.
- 791 Evanno G, Regnaut S, Goudet J. 2005. Detecting the number of clusters of individuals using the
792 software STRUCTURE: a simulation study. *Mol. Ecol.* 14:2611–2620.
- 793 Feng L-Y, Yan B-B, Huang Y-Z, Li L. 2021. Abnormal methylation characteristics predict
794 chemoresistance and poor prognosis in advanced high-grade serous ovarian cancer. *Clin.*
795 *Epigenetics.* 13:141.
- 796 Flores KB, Wolschin F, Amdam GV. 2013. The role of methylation of DNA in environmental
797 adaptation. *Integr. Comp. Biol.* 53:359–372.
- 798 Foll M, Gaggiotti O. 2008. A genome-scan method to identify selected loci appropriate for both
799 dominant and codominant markers: A Bayesian perspective. *Genetics.* 180:977–993.
- 800 Gao X, Thomsen H, Zhang Y, Breitling LP, Brenner H. 2017. The impact of methylation
801 quantitative trait loci (mQTLs) on active smoking-related DNA methylation changes. *Clin.*
802 *Epigenetics.* 9:87.
- 803 Gavery MR, Roberts SB. 2013. Predominant intragenic methylation is associated with gene
804 expression characteristics in a bivalve mollusc. *PeerJ.* 1:e215.
- 805 Giraud G, Terrone S, Bourgeois CF. 2018. Functions of DEAD box RNA helicases DDX5 and
806 DDX17 in chromatin organization and transcriptional regulation. *BMB Rep.* 51:613–622.
- 807 Gonzalez-Romero R et al. 2017. Effects of Florida Red Tides on histone variant expression and
808 DNA methylation in the Eastern oyster *Crassostrea virginica*. *Aquat. Toxicol.* 186:196–204.
- 809 Gracey AY et al. 2008. Rhythms of gene expression in a fluctuating intertidal environment. *Curr.*

- 810 Biol. 18:1501–1507.
- 811 Haider S et al. 2016. A bedr way of genomic interval processing. *Source Code Biol. Med.* 11:14.
- 812 Heare JE, Blake B, Davis JP, Vadopalas B, Roberts SB. 2017. Evidence of *Ostrea lurida*
813 Carpenter, 1864, population structure in Puget Sound, WA, USA. *Mar. Ecol.* 38:e12458.
- 814 Heare JE, White SJ, Vadopalas B, Roberts SB. 2018. Differential response to stress in *Ostrea*
815 *lurida* as measured by gene expression. *PeerJ.* 6:e4261.
- 816 Héberlé É, Bardet AF. 2019. Sensitivity of transcription factors to DNA methylation. *Essays*
817 *Biochem.* 63:727–741.
- 818 Heyn H et al. 2013. DNA methylation contributes to natural human variation. *Genome Res.*
819 23:1363–1372.
- 820 Huang DW, Sherman BT, Lempicki RA. 2009. Systematic and integrative analysis of large gene
821 lists using DAVID bioinformatics resources. *Nat. Protoc.* 4:44–57.
- 822 Husquin LT et al. 2018. Exploring the genetic basis of human population differences in DNA
823 methylation and their causal impact on immune gene regulation. *Genome Biol.* 19:222.
- 824 Jaenisch R, Bird A. 2003. Epigenetic regulation of gene expression: how the genome integrates
825 intrinsic and environmental signals. *Nat. Genet.* 33 Suppl:245–254.
- 826 Jeffery L, Nakielny S. 2004. Components of the DNA methylation system of chromatin control
827 are RNA-binding proteins. *J. Biol. Chem.* 279:49479–49487.
- 828 Jiang Q, Li Q, Yu H, Kong LF. 2013. Genetic and epigenetic variation in mass selection
829 populations of Pacific oyster *Crassostrea gigas*. *Genes Genomics.* 35:641-647.
- 830 Johnson KM, Kelly MW. 2020. Population epigenetic divergence exceeds genetic divergence in
831 the Eastern oyster *Crassostrea virginica* in the Northern Gulf of Mexico. *Evol. Appl.* 77:205799.
- 832 Johnson KM, Sirovy KA, Casas SM, La Peyre JF, Kelly MW. 2020. Characterizing the
833 Epigenetic and Transcriptomic Responses to *Perkinsus marinus* Infection in the Eastern Oyster
834 *Crassostrea virginica*. *Frontiers in Marine Science.*
- 835 Kawamura K, Miyake T, Obata M, Aoki H, Komaru A. 2017. Population demography and
836 genetic characteristics of the Pacific Oyster *Crassostrea gigas* in Japan. *Biochem. Syst. Ecol.*
837 70:211–221.
- 838 Khangaonkar T et al. 2018. Analysis of Hypoxia and Sensitivity to Nutrient Pollution in Salish
839 Sea. *J. Geophys. Res. C: Oceans.* 123:4735–4761.
- 840 Kimura M. 1983. *The Neutral Theory of Molecular Evolution*. Cambridge University Press.
- 841 Klironomos FD, Berg J, Collins S. 2013. How epigenetic mutations can affect genetic evolution:
842 model and mechanism. *Bioessays.* 35:571–578.
- 843 Kopelman NM, Mayzel J, Jakobsson M, Rosenberg NA, Mayrose I. 2015. CLUMPAK: A
844 program for identifying clustering modes and packaging population structure inferences across

845 K. *Mol. Ecol. Resour.* 15:1179–1191.

846 Korneliussen TS, Albrechtsen A, Nielsen R. 2014. ANGSD: Analysis of Next Generation
847 Sequencing Data. *BMC Bioinformatics.* 15:356.

848 Krueger F. 2012. Trim Galore: a wrapper tool around Cutadapt and FastQC to consistently
849 apply quality and adapter trimming to FastQ files, with some extra functionality for MspI-
850 digested RRBS-type (Reduced Representation Bisulfite-Seq) libraries. URL [http://www.](http://www.bioinformatics.babraham.ac.uk/projects/trim_galore/)
851 [bioinformatics.babraham.ac.uk/projects/trim_galore/](http://www.bioinformatics.babraham.ac.uk/projects/trim_galore/). (Date of access: 28/04/2016).

852 Krueger F, Andrews SR. 2011. Bismark: a flexible aligner and methylation caller for Bisulfite-
853 Seq applications. *Bioinformatics.* 27:1571–1572.

854 Kvist J et al. 2018. Pattern of DNA Methylation in *Daphnia*: Evolutionary Perspective. *Genome*
855 *Biol. Evol.* 10:1988–2007.

856 Langmead B, Salzberg SL. 2012. Fast gapped-read alignment with Bowtie 2. *Nat. Methods.*
857 9:357–359.

858 Lienert F et al. 2011. Identification of genetic elements that autonomously determine DNA
859 methylation states. *Nat. Genet.* 43:1091–1097.

860 Liew YJ et al. 2018. Epigenome-associated phenotypic acclimatization to ocean acidification in
861 a reef-building coral. *Sci Adv.* 4:eaar8028.

862 Liew YJ et al. 2020. Intergenerational epigenetic inheritance in reef-building corals. *Nat. Clim.*
863 *Chang.* 10:254–259.

864 Li H et al. 2009. The Sequence Alignment/Map format and SAMtools. *Bioinformatics.* 25:2078–
865 2079.

866 Li J et al. 2015. Cloning and characterization of three suppressors of cytokine signaling (SOCS)
867 genes from the Pacific oyster, *Crassostrea gigas*. *Fish Shellfish Immunol.* 44:525–532.

868 Li J et al. 2012. Genomic hypomethylation in the human germline associates with selective
869 structural mutability in the human genome. *PLoS Genet.* 8:e1002692.

870 Lim Y-K et al. 2020. DNA methylation changes in response to ocean acidification at the time of
871 larval metamorphosis in the edible oyster, *Crassostrea hongkongensis*. *Mar. Environ. Res.*
872 163:105217.

873 Lipkin SM et al. 2000. MLH3: a DNA mismatch repair gene associated with mammalian
874 microsatellite instability. *Nat. Genet.* 24:27–35.

875 Lowry DB et al. 2017. Responsible RAD: Striving for best practices in population genomic
876 studies of adaptation. *Mol. Ecol. Resour.* 17:366–369.

877 Lyko F et al. 2010. The honey bee epigenomes: differential methylation of brain DNA in queens
878 and workers. *PLoS Biol.* 8:e1000506.

879 Martin M. 2011. Cutadapt removes adapter sequences from high-throughput sequencing reads.
880 *EMBnet.journal.* 17:10–12.

881 Martin-Trujillo A et al. 2020. Rare genetic variation at transcription factor binding sites
882 modulates local DNA methylation profiles. *PLoS Genet.* 16:e1009189.

883 Maynard A, Bible JM, Pespeni MH, Sanford E, Evans TG. 2018. Transcriptomic responses to
884 extreme low salinity among locally adapted populations of Olympia oyster (*Ostrea lurida*). *Mol.*
885 *Ecol.* 27:4225–4240.

886 McCaw ZR, Lane JM, Saxena R, Redline S, Lin X. 2020. Operating characteristics of the rank-
887 based inverse normal transformation for quantitative trait analysis in genome-wide association
888 studies. *Biometrics.* 76:1262–1272.

889 McClay JL et al. 2015. High density methylation QTL analysis in human blood via next-
890 generation sequencing of the methylated genomic DNA fraction. *Genome Biol.* 16:291.

891 de Mendoza A, Lister R, Bogdanovic O. 2019. Evolution of DNA Methylome Diversity in
892 Eukaryotes. *J. Mol. Biol.* doi: 10.1016/j.jmb.2019.11.003.

893 Moore SK et al. 2008. A descriptive analysis of temporal and spatial patterns of variability in
894 Puget Sound oceanographic properties. *Estuar. Coast. Shelf Sci.* 80:545–554.

895 Nitta KR et al. 2015. Conservation of transcription factor binding specificities across 600 million
896 years of bilateria evolution. *Elife.* 4. doi: 10.7554/eLife.04837.

897 Olson CE, Roberts SB. 2014. Genome-wide profiling of DNA methylation and gene expression
898 in *Crassostrea gigas* male gametes. *Front. Physiol.* 5:224.

899 Ozato K, Shin D-M, Chang T-H, Morse HC 3rd. 2008. TRIM family proteins and their emerging
900 roles in innate immunity. *Nat. Rev. Immunol.* 8:849–860.

901 Park J et al. 2011. Comparative analyses of DNA methylation and sequence evolution using
902 *Nasonia* genomes. *Mol. Biol. Evol.* 28:3345–3354.

903 Pritchard C, Shanks A, Rimler R, Oates M, Rumrill S. 2015. The Olympia oyster *Ostrea lurida*:
904 Recent advances in natural history, ecology, and restoration. *J. Shellfish Res.* 34. doi:
905 10.2983/035.034.0207.

906 Quinlan AR. 2014. BEDTools: The Swiss-Army Tool for Genome Feature Analysis. *Curr. Protoc.*
907 *Bioinformatics.* 47:11.12.1–34.

908 Reynolds J, Weir BS, Cockerham CC. 1983. Estimation of the coancestry coefficient: basis for a
909 short-term genetic distance. *Genetics.* 105:767–779.

910 Rivière G. 2014. Epigenetic features in the oyster *Crassostrea gigas* suggestive of functionally
911 relevant promoter DNA methylation in invertebrates. *Front. Physiol.* 5:129.

912 Roberts SB, Gavery MR. 2012. Is There a Relationship between DNA Methylation and
913 Phenotypic Plasticity in Invertebrates? *Front. Physiol.* 2:116.

914 Sanford E, Kelly MW. 2011. Local adaptation in marine invertebrates. *Ann. Rev. Mar. Sci.*
915 3:509–535.

916 Schmid MW et al. 2018. Contribution of epigenetic variation to adaptation in *Arabidopsis*. *Nature*

- 917 Communications. 9. doi: 10.1038/s41467-018-06932-5.
- 918 Schoch GC et al. 2006. Fifteen degrees of separation: Latitudinal gradients of rocky intertidal
919 biota along the California Current. *Limnol. Oceanogr.* 51:2564–2585.
- 920 Schorderet DF, Gartler SM. 1992. Analysis of CpG suppression in methylated and
921 nonmethylated species. *Proc. Natl. Acad. Sci. U. S. A.* 89:957–961.
- 922 Shabalin AA. 2012. Matrix eQTL: ultra fast eQTL analysis via large matrix operations.
923 *Bioinformatics.* 28:1353–1358.
- 924 Shabalin AA et al. 2018. RaMWAS: fast methylome-wide association study pipeline for
925 enrichment platforms. *Bioinformatics.* 34:2283–2285.
- 926 Shanks AL. 2009. Pelagic larval duration and dispersal distance revisited. *Biol. Bull.* 216:373–
927 385.
- 928 Shoemaker R, Deng J, Wang W, Zhang K. 2010. Allele-specific methylation is prevalent and is
929 contributed by CpG-SNPs in the human genome. *Genome Res.* 20:883–889.
- 930 Silliman K. 2019. Population structure, genetic connectivity, and adaptation in the Olympia
931 oyster (*Ostrea lurida*) along the west coast of North America. *Evol. Appl.* 11:697.
- 932 Silliman KE, Bowyer TK, Roberts SB. 2018. Consistent differences in fitness traits across
933 multiple generations of Olympia oysters. *Sci. Rep.* 8:6080.
- 934 Skinner MK et al. 2014. Epigenetics and the evolution of Darwin's Finches. *Genome Biol. Evol.*
935 6:1972–1989.
- 936 Skotte L, Korneliussen TS, Albrechtsen A. 2013. Estimating individual admixture proportions
937 from next generation sequencing data. *Genetics.* 195:693–702.
- 938 Song K. 2020. Genomic Landscape of Mutational Biases in the Pacific Oyster *Crassostrea*
939 *gigas*. *Genome Biol. Evol.*
- 940 Song K, Li L, Zhang G. 2017. The association between DNA methylation and exon expression
941 in the Pacific oyster *Crassostrea gigas*. *PLoS One.* 12:e0185224.
- 942 Spencer LH et al. 2020. Carryover effects of temperature and pCO₂ across multiple Olympia
943 oyster populations. *Ecol. Appl.* 30:e02060.
- 944 Suzuki MM, Bird A. 2008. DNA methylation landscapes: provocative insights from epigenomics.
945 *Nat. Rev. Genet.* 9:465–476.
- 946 Takeuchi M et al. 2003. The prickle-related gene in vertebrates is essential for gastrulation cell
947 movements. *Curr. Biol.* 13:674–679.
- 948 Taudt A, Colomé-Tatché M, Johannes F. 2016. Genetic sources of population epigenomic
949 variation. *Nat. Rev. Genet.* 17:319–332.
- 950 Timmins-Schiffman EB, Friedman CS, Metzger DC, White SJ, Roberts SB. 2013. Genomic
951 resource development for shellfish of conservation concern. *Mol. Ecol. Resour.* 13:295–305.

- 952 Trigg SA et al. 2021. Invertebrate methylomes provide insight into mechanisms of
953 environmental tolerance and reveal methodological biases. *Mol. Ecol. Resour.* doi:
954 10.1111/1755-0998.13542.
- 955 Varriale A. 2014. DNA methylation, epigenetics, and evolution in vertebrates: facts and
956 challenges. *Int. J. Evol. Biol.* 2014:475981.
- 957 Venkataraman YR et al. 2020. General DNA Methylation Patterns and Environmentally-Induced
958 Differential Methylation in the Eastern Oyster (*Crassostrea virginica*). *Frontiers in Marine*
959 *Science.* 7:225.
- 960 Vieira FG, Lassalle F, Korneliussen TS. 2016. Improving the estimation of genetic distances
961 from Next-Generation Sequencing data. *Biol. J. Linn. Soc. Lond.*
962 <https://academic.oup.com/biolinnean/article-abstract/117/1/139/2440246>.
- 963 Wagner JR et al. 2014. The relationship between DNA methylation, genetic and expression
964 inter-individual variation in untransformed human fibroblasts. *Genome Biol.* 15:R37.
- 965 Wang H-Q, Tuominen LK, Tsai C-J. 2011. SLIM: a sliding linear model for estimating the
966 proportion of true null hypotheses in datasets with dependence structures. *Bioinformatics.*
967 27:225–231.
- 968 Wang S, Meyer E, McKay JK, Matz MV. 2012. 2b-RAD: a simple and flexible method for
969 genome-wide genotyping. *Nat. Methods.* 9:808–810.
- 970 Wang X et al. 2020. DNA methylation mediates differentiation in thermal responses of Pacific
971 oyster (*Crassostrea gigas*) derived from different tidal levels. *Heredity* . doi: 10.1038/s41437-
972 020-0351-7.
- 973 Wang X et al. 2014. Genome-wide and single-base resolution DNA methylomes of the Pacific
974 oyster *Crassostrea gigas* provide insight into the evolution of invertebrate CpG methylation.
975 *BMC Genomics.* 15:1119. doi: 10.1186/1471-2164-15-1119.
- 976 Wang X, Li A, Wang W, Zhang G, Li L. 2021a. Direct and heritable effects of natural tidal
977 environments on DNA methylation in Pacific oysters (*Crassostrea gigas*). *Environmental*
978 *Research.* 111058. doi: 10.1016/j.envres.2021.111058.
- 979 Wang X, Li A, Wang W, Zhang G, Li L. 2021b. Direct and heritable effects of natural tidal
980 environments on DNA methylation in Pacific oysters (*Crassostrea gigas*). *Environ. Res.*
981 197:111058.
- 982 Weersing K, Toonen RJ. 2009. Population genetics, larval dispersal, and connectivity in marine
983 systems. *Mar. Ecol. Prog. Ser.* 393:1–12.
- 984 White SJ, Vadopalas B, Silliman K, Roberts SB. 2017. Genotype-by-sequencing of three
985 geographically distinct populations of Olympia oysters, *Ostrea lurida*. *Sci Data.* 4:170130.
- 986 Wickham H. 2016. *ggplot2: Elegant Graphics for Data Analysis*. Springer-Verlag New York.
- 987 Wolf DA, Lin Y, Duan H, Cheng Y. 2020. eIF-Three to Tango: emerging functions of translation
988 initiation factor eIF3 in protein synthesis and disease. *J. Mol. Cell Biol.* 12:403–409.

- 989 Yang W et al. 2020. ddRADseq-assisted construction of a high-density SNP genetic map and
990 QTL fine mapping for growth-related traits in the spotted scat (*Scatophagus argus*). *BMC*
991 *Genomics*. 21:278.
- 992 Zemach A, McDaniel IE, Silva P, Zilberman D. 2010. Genome-wide evolutionary analysis of
993 eukaryotic DNA methylation. *Science*. 328:916–919.
- 994 Zhang J, Luo S, Gu Z, Deng Y, Jiao Y. 2020. Genome-wide DNA Methylation Analysis of Mantle
995 Edge and Mantle Central from Pearl Oyster *Pinctada fucata martensii*. *Mar. Biotechnol.* .
996 22:380–390.
- 997 Zhang X, Li Q, Kong L, Yu H. 2017. DNA methylation changes detected by methylation-
998 sensitive amplified polymorphism in the Pacific oyster (*Crassostrea gigas*) in response to salinity
999 stress. *Genes Genomics*. 39:1173–1181.
- 1000 Zhang X, Li Q, Kong L, Yu H. 2018. Epigenetic variation of wild populations of the Pacific oyster
1001 *Crassostrea gigas* determined by methylation-sensitive amplified polymorphism analysis. *Fish.*
1002 *Sci*. 84:61–70.
- 1003 Zhang X, Li Q, Yu H, Kong L. 2017. Effects of air exposure on genomic DNA methylation in the
1004 Pacific oyster (*Crassostrea gigas*). *Zhongguo Shui Chan Ke Xue*. 24:690–697.
- 1005 Zhi D et al. 2013. SNPs located at CpG sites modulate genome-epigenome interaction.
1006 *Epigenetics*. 8:802–806.

1007 Data Availability Statement

1008 Code and intermediate analysis files used in this study are available in the accompanying
1009 repository <https://github.com/sr320/paper-oly-mbdbbs-gen>. The genome assembly can be found
1010 at NCBI under the accession PRJEB39287. The annotation files used for these analyses and
1011 raw data for the genome assembly will be made available upon publication. Raw 2b-RAD data
1012 and MBD-BS data will be available on NCBI Sequence Read Archive by time of submission.